Effect of Packaging Method on Performance of Light-Emitting Diodes With Quantum Dot Phosphor

Bin Xie, Run Hu, Xingjian Yu, Bofeng Shang, Yupu Ma, and Xiaobing Luo, *Senior Member, IEEE*

***Abstract*—In this letter, remote quantum dot phosphor-converted light-emitting diodes (QD-LEDs) with air encapsulation, silicone lens, and silicone encapsulation were fabricated. The effects of different packaging methods on the optical and thermal performances of QD-LEDs were evaluated based on the experimental tests and simulation. Optical efficiency and spectral stability were tested by experiment, and the temperature was assessed by finite-element simulation and infrared thermal imager tests. It was found that the silicone encapsulation type could convert more blue light into QDs emission light due to the reabsorption of backward reflected blue light. The silicone encapsulation type showed only a 6.2% decrease in QDs emission peak intensity when the driving current varied from 50 to 500 mA, while the silicone lens type dropped by 20.4% and the air encapsulation dropped by 36.8%. It was also confirmed that the QDs temperature in silicone encapsulation was 24 °C lower than those in the air encapsulation type and the silicone lens type at driving current of 300 mA.**

***Index Terms*—Light emitting diodes, quantum dots, thin film devices.**

I. INTRODUCTION

WHITE light-emitting diodes (wLEDs) have been considered as promising light sources with extraordinary characteristics of high luminous efficiency, low power consumption, long lifetime and low environmental impact [1]–[3]. Currently, the phosphor-converted LEDs (pcLEDs) are the most-widely used wLEDs due to their high efficiency and reliability. However, the color rendering index (CRI) of pcLEDs is quite low owing to the lack of red component in the emission spectrum. To overcome this shortcoming, inorganic polymer [4], [5], OLED material [6] and quantum dots (QDs) [7], [8] have been considered as the alternatives to generate white light based on blue LEDs. Among these materials, semiconductor QDs are regarded as promising candidates due to their high quantum yield, narrow emission band and tunable band gap. QD particles are usually embedded in colloid to fabricate the QD-polymer film, which is then combined with a blue LED chip to generate the quantum dot phosphor-converted LEDs (QD-LEDs).

In the photoluminescent process, due to the lower radiative recombination efficiency of QDs than phosphor, QDs generate more heat than phosphors and results in higher temperature rise in QD-LEDs [9]. In consequence, the optical efficiency of colloidal QDs drops due to its poor temperature stability. To relieve this thermal problem, remote type packaging was widely adopted in QD-LEDs to avoid direct contact between LED chip and QD-polymer film. Analog to the packaging structures of phosphor glass [10]–[12], there are three types of frequently-used remote QD-LEDs, i.e. air encapsulation (Type 1) [13], silicone lens (Type 2) [14], and silicone encapsulation (Type 3) [15], which are shown in Fig. 1. In Type 1, the inner space between QD-polymer film and LED chip is filled with air. In Type 2, a silicone lens is coated on the LED chip, while in Type 3, silicone gel is filled into the space between QD-polymer film and LED chip. The blue light emitted from the LED chip stimulates the QD-polymer film to generate red, green, or yellow emission, which mix with the transmitted blue light and finally generate white light. Based on the experience in conventional LED packaging, it is perceived that the packaging structure of QD-LEDs influences the optical performance greatly as well [16]. However, few studies refer to this problem of QD-LEDs by experiments or simulations. Shin *et al.* [14] compared the optical performance of Types 2 and 3, and they concluded that the optical extraction efficiency of Type 2 was higher than that of Type 3 by 29.7%. It was also observed that the correlated color temperature (CCT) of these two types differed greatly, which indicates that the corresponding spectra were different in the two packaging types. Besides, their conclusion was obtained by transient optical analysis and measurement, and the fundamental mechanism behind their results was not presented in detail.

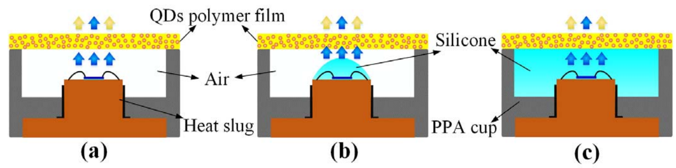

Fig. 1. Three frequently-used configurations of QD-LEDs package with (a) air encapsulation, (b) silicone lens and (c) silicone encapsulation.

In this letter, we evaluated the effect of different packaging methods on the optical and thermal performances of QD-LEDs through both experiments and simulations. Three types of remote QD-LEDs shown in Fig.1 were fabricated. Their light extraction efficiency as well as the luminous efficiency were compared and analyzed. The heat generated by the LED chip and the QD-polymer film was assessed, and the resulting

Manuscript received January 6, 2016; revised January 27, 2016; accepted February 15, 2016. Date of publication February 18, 2016; date of current version March 29, 2016. This work was supported by the National Science Foundation of China under Grant 51376070 and Grant 51576078.

The authors are with the State Key Laboratory of Coal Combustion, School of Energy and Power Engineering, Huazhong University of Science and Technology, Wuhan, 430074, China. (e-mail: luoxb@hust.edu.cn).

Color versions of one or more of the figures in this letter are available online at http://ieeexplore.ieee.org.

Digital Object Identifier 10.1109/LPT.2016.2531794

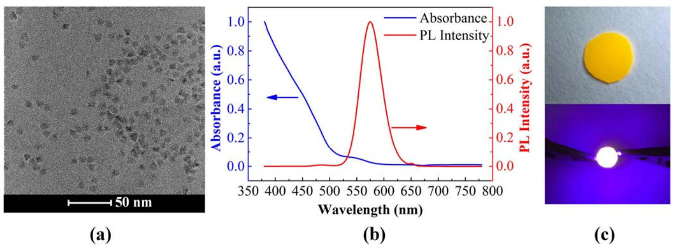

Fig. 2. (a) High resolution TEM image of CdSSe/ZnS QDs. (b) Normalized absorption and photoluminescence spectra of CdSSe/ZnS QDs. (c) QD-polymer film (upper), and the QD-LEDs under 300 mA (lower).

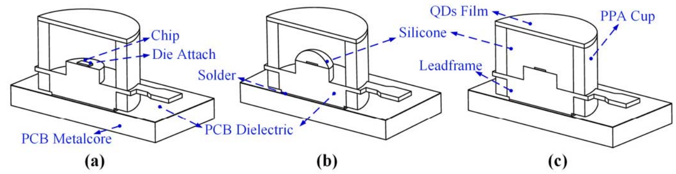

Fig. 3. FEM model of QD-LEDs packages with (a) air encapsulation, (b) silicone lens and (c) silicone encapsulation.

temperature was estimated by thermal simulations. Detailed analyses of the relation between temperature fields and the optical performance of QD-LEDs are presented as well.

II. Preparation, Test and Simulation Methods

In the first step, we fabricated the remote QD-polymer film. CdSSe/ZnS core-shell quantum dots (L05-10, Najingtech Inc.) were chosen as the down-converting material. Fig. 2(a) illustrates the high-resolution Transmission Electron Microscope (TEM) image of this inorganic passivated QDs whose average size is 6.7 nm. Fig. 2(b) shows the UV-visible absorption and photoluminescence (PL) spectra of CdSSe/ZnS, with peak emission wavelength of 574 nm and full width at half maximum (FWHM) of 32 nm. To fabricate the QD-polymer film, 2 mg of CdSSe/ZnS QDs were firstly dissolved in chloroform, and then mixed with 1g of polymethylmethacrylate (PMMA)-chloroform solution. The mixed solution was poured into a teflon mould, and then placed in a vacuum chamber to remove the chloroform and bubbles. Composite QD-polymer film was fabricated after the chloroform was volatilized. Then silicone gel (OE6550, A: B=1: 1, Dow Corning) was dispensed on the bare modules to form the corresponding silicone lens type and silicone encapsulation type, then the QD-polymer film was coated on the top of LED module. After that, the whole module was cured at 90 °C for 1h. Fig. 2(c) shows the fabricated QD-polymer film and the QD-LEDs with silicone encapsulation under 300 mA.

The optical properties including luminous efficiency and spectral stability with varying driving currents of these three packages were measured by an integrating sphere (ATA-1000, EVERFINE Inc.). According to the optical energy losses of QD-LEDs, the heat generation of LED chip (Q_{Chip}) and QDs polymer film (Q_{QDs}) were calculated as follows:

$$Q_{Chip} = P_{El} - P_{Op,ref} \quad (1)$$

$$Q_{QDs} = P_{Op,ref} - P_{Op} \quad (2)$$

where P_{El} is the input electric power from QD-LEDs package, P_{Op} is the optical power from the QD-LEDs package, and $P_{Op,ref}$ is the measured optical power from the bare package filled with air or silicone without QD-polymer film. It is assumed that the entire optical power loss is converted into heat in the QD-polymer film [17].

To conduct the thermal simulation, we built three corresponding QD-LEDs models, as shown in Fig. 3. The LED module was mounted on a metal-core printed circuit board (MCPCB) for electrical connection and heat dissipation. Inside the LED module, a blue LED chip was mounted onto a lead-frame via die attach adhesive. The lead-frame was soldered onto the PCB. Thickness and thermal conductivity of the different layers used in the simulation are listed in Table 1. The heat generations of chip and QDs from Eqs. (1) and (2) were loaded on the finite element model and then the thermal simulation was conducted.

TABLE I
Thickness and Thermal Conductivity of the Packaging Materials in Thermal Simulation

Layer	Thickness (mm)	Thermal Conductivity (W/m·K)
LED Chip	0.1	65.6
Die Attach	0.02	5
Lead-frame	2.5	170
Solder	0.1	5
PPA Cup	4.5	0.36
PCB Dielectric	0.03	0.2
Silicone	1.5	0.3
QD-polymer film	0.3	0.4

In the FEM simulation, only a quarter of the QD-LEDs model was utilized to simulate the temperature field, due to its symmetry. The boundary conditions of the FEM model were set as follows: the ambient temperature was fixed at 25°C; forced convection occurred at the bottom surface of the PCB with a heat transfer coefficient of 30 W/(m^2·K), and other surfaces are cooled by convection with a heat transfer coefficient of 10 W/(m^2·K). All the boundary conditions were the same as those in [18].

III. Results and Discussions

Fig. 4 shows the current-dependent optical power and luminous efficiency of the three QD-LEDs when the driving current varies from 50 mA to 500 mA. Here the optical power of QD-LEDs is defined as the integration of spectrum intensity over the spectrum from 380 nm to 780 nm, while the QDs emission power is defined as the integration from 520 nm to 780 nm. Type 2 QD-LEDs showed the highest optical power, which was 3.8% higher than Type 3 and 16.4% higher than Type 1 at driving current of 300 mA. The inset in Fig. 4(a) shows the QDs emission power. The QDs emission power in Type 3 was higher than that in other two types. Consequently, although the optical power of Type 3 was lower than that of Type 2,

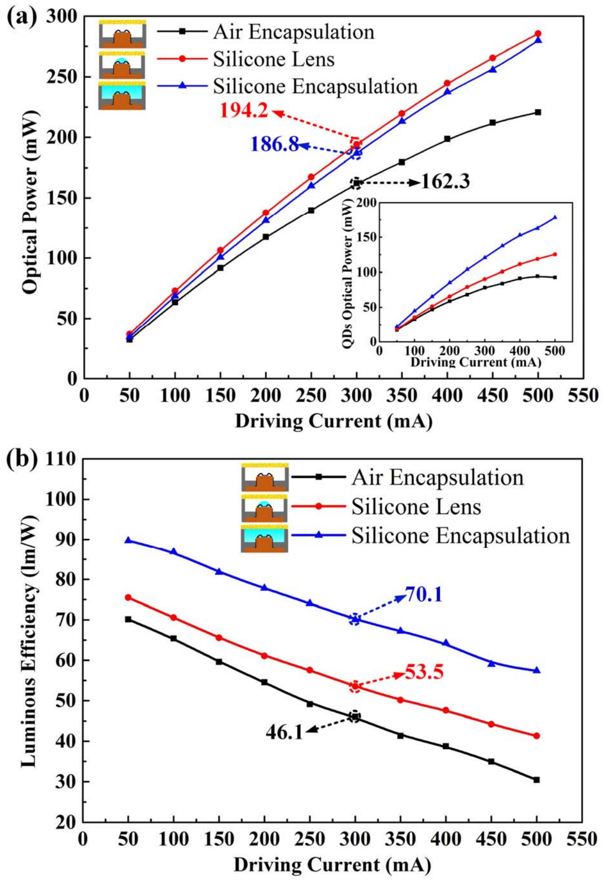

Fig. 4. (a) Optical power and (b) luminous efficiency of the three QD-LEDs at varying driving current from 50 mA to 500 mA. The inset in Fig. 4(a) shows the QDs emission power of the three QD-LEDs.

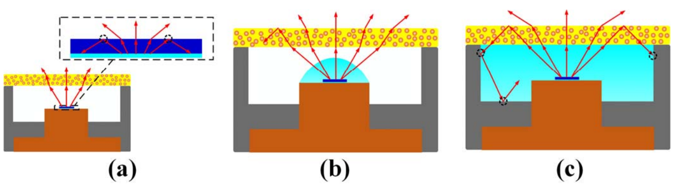

Fig. 5. Schematic illustration of the light output mechanism of three QD-LEDs: (a) air encapsulation, (b) silicone lens and (c) silicone encapsulation.

Type 3 achieved a higher luminous efficiency, which was 31% higher than Type 2 and 52% higher than Type 1 at 300 mA, as shown in Fig. 4(b).

Fig. 5 shows the schematic illustration of the light output mechanism of the three packages. Fig. 5(a) visualizes that many total internal reflection (TIR) incidents occur at the interface between the LED chip and air, resulting in lower optical power and luminous efficiency. For Type 2 (Fig. 5(b)), some rays in the QDs layer are scattered and reemitted backward. Due to the air layer between QDs layer and silicone lens, a significant portion of the downward rays would be reflected at the air-QDs layer interface and finally exit the QDs layer. For Type 3, some of the downward rays would be absorbed by the PPA cup, and most of them would be reflected upward to

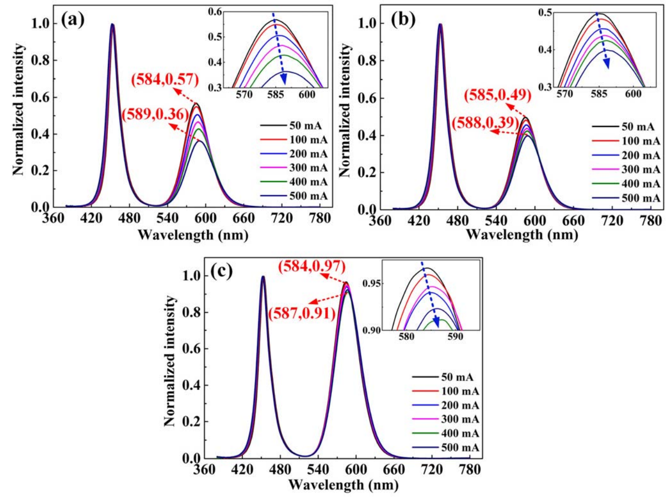

Fig. 6. Normalized emission spectra of the three types of QD-LEDs packages at varying driving current: (a) Air encapsulation type, (b) silicone lens type and (c) silicone encapsulation type. The insets show the details of QDs emission peak.

the QDs again. Therefore, Type 3 QD-LEDs show less optical power but more QDs emission. Both our results and those in [14] predict the same trend that the optical power of Type 2 is higher than that of Type 3, while there are differences in the absolute values of optical efficiency enhancement. This can be attributed to the difference in packaging structure as well as the surface reflection. Furthermore, according to the eye sensitivity function, equivalent power of blue light from LED chip results in less luminous efficiency than QD-emitted green or yellow light. More QDs emission results in higher luminous efficiency. Therefore, though Type 3 showed lower optical power than Type 2, Type 3 QD-LEDs possessed higher luminous efficiency.

In order to better understand the relationship between luminous efficiency and emission spectra, the emission spectra of three types of QD-LEDs packages at different driving currents were measured. Fig. 6 shows the normalized emission spectra of three packages when the driving current varied from 50 mA to 500 mA. It was found that the peak emission intensity of QDs emission in the three packages was much different. Type 3 showed the highest QDs emission intensity as well as the highest QDs emission power. When the driving current increased from 50 mA to 500 mA, the peak emission intensity of Type 1 dropped by 36.8% and Type 2 dropped by 20.4%, while Type 3 only dropped by 6.2%. Since the QDs emission is related to its temperature [19]–[21], we simulated the temperature fields of these QD-LEDs to explore the reasons behind these spectral characteristics.

Fig. 7 shows the temperature fields of these three packages under driving current of 300 mA. From the maximum and minimum temperature of the whole package marked in Fig. 7, it was seen that the highest temperatures of all the packages locate in the QD-polymer film, which implies that QDs temperature is higher than chip temperature in the remote QD-LEDs. Further, the highest QDs temperature in the Type 3 was 24°C lower than that in Type 1 and Type 2.

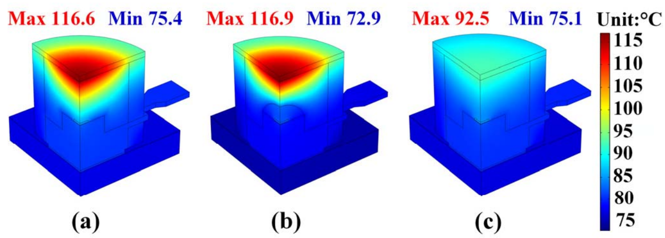

Fig. 7. Simulated temperature fields of the three QD-LEDs packages under driving current of 300 mA: (a) Air encapsulation type, (b) silicone lens type and (c) silicone encapsulation type.

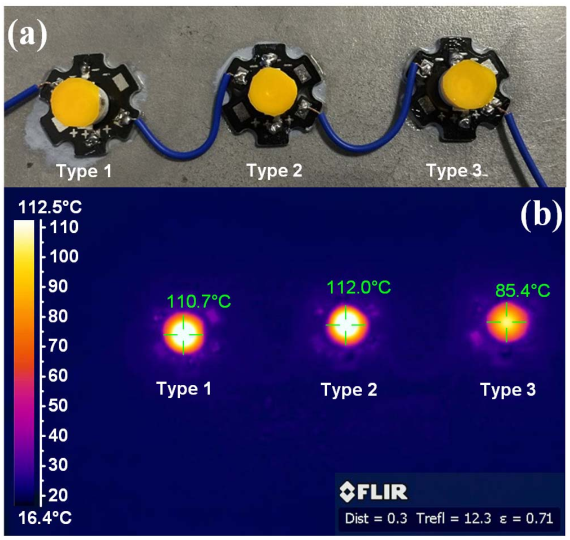

Fig. 8. (a) Image of the three QD-LEDs packages. (b) Temperature fields of three QD-LEDs packages measured by infrared thermal imager.

Furthermore, to validate the simulated temperature fields, we measured the corresponding temperature fields of these three packages by infrared imaging. As shown in Fig. 8(a), these three QD-LEDs were mounted on a PCB separately, and driven by the same current of 300 mA. After temperature stabilization, the temperature fields of these packages were obtained by an infrared thermal imager (FLIR SC620), as shown in Fig. 8(b). It is seen from the experimental data that the maximum temperature of QD-polymer film in Types 1, 2 and 3 are 110.7°C, 112.0°C and 85.4°C, respectively. The simulated temperature differences among these three packages agree well with the experiments. Since the non-radiative recombination due to traps on the surface of the QDs increased with temperature, causing the thermal quenching effect [20], the lower temperature of the silicone encapsulation type is an important reason for its superior spectral stability.

IV. Conclusions

This letter discussed the optical performances and thermal characteristics of three types of frequently-used remote QD-LEDs. By combining experimental measurement results with FEM simulation, the light output efficiency, spectra, spectral stability as well as the temperature fields of three different types of QD-LEDs were obtained and analyzed. It was found that the silicone encapsulation type could convert more blue light into QDs emission light due to the reabsorption of backward blue light, and the silicone encapsulation type shows the highest spectral stability. The QDs temperature of the silicone encapsulation type was lower than other two types, which is an important reason for its superior spectral stability.

References

[1] S. Pimputkar, J. S. Speck, S. P. DenBaars, and S. Nakamura, "Prospects for LED lighting," *Nature Photon.*, vol. 3, no. 4, pp. 180–182, Apr. 2009.

[2] C. Yuan, L. Li, B. Duan, B. Xie, Y. Zhu, and X. Luo, "Locally reinforced polymer-based composites for efficient heat dissipation of local heat source," *Int. J. Thermal Sci.*, vol. 102, pp. 202–209, Apr. 2016.

[3] C. Yuan, B. Xie, M. Huang, R. Wu, and X. Luo, "Thermal conductivity enhancement of platelets aligned composites with volume fraction from 10% to 20%," *Int. J. Heat Mass Transf.*, vol. 94, pp. 20–28, Mar. 2016.

[4] M. Nazarov, D. Y. Noh, J. Sohn, and C. Yoon, "Influence of additional Eu^{3+} coactivator on the luminescence properties of $Tb_3Al_5O_{12}$:Ce^{3+}, Eu^{3+}," *Opt. Mater.*, vol. 30, no. 9, pp. 1387–1392, May 2008.

[5] B. Kokuoz, C. Kucera, J. R. DiMaio, and J. Ballato, "Organic–inorganic hybrid nanoparticles with enhanced rare-earth emissions," *Opt. Mater.*, vol. 31, no. 9, pp. 1327–1330, Jul. 2009.

[6] M. C. Gather, A. Köhnen, and K. Meerholz, "White organic light-emitting diodes," *Adv. Mater.*, vol. 23, no. 2, pp. 233–248, Oct. 2010.

[7] E. Jang, S. Jun, H. Jang, J. Lim, B. Kim, and Y. Kim, "White-light-emitting diodes with quantum dot color converters for display backlights," *Adv. Mater.*, vol. 22, no. 28, pp. 3076–3080, Jul. 2010.

[8] W.-S. Song and H. Yang, "Efficient white-light-emitting diodes fabricated from highly fluorescent copper indium sulfide core/shell quantum dots," *Chem. Mater.*, vol. 24, no. 10, pp. 1961–1967, May 2012.

[9] J. Y. Woo, K. N. Kim, S. Jeong, and C.-S. Han, "Thermal behavior of a quantum dot nanocomposite as a color converting material and its application to white LED," *Nanotechnology*, vol. 21, no. 49, p. 495704, Dec. 2010.

[10] S. Wang, X. Chen, M. Chen, H. Zheng, H. Yang, and S. Liu, "Improvement in angular color uniformity of white light-emitting diodes using screen-printed multilayer phosphor-in-glass," *Appl. Opt.*, vol. 53, no. 36, pp. 8492–8498, Dec. 2014.

[11] L.-Y. Chen, W.-C. Cheng, C.-C. Tsai, Y.-C. Huang, Y.-S. Lin, and W.-H. Cheng, "High-performance glass phosphor for white-light-emitting diodes via reduction of Si-Ce^{3+}:YAG inter-diffusion," *Opt. Mater. Exp.*, vol. 4, no. 1, pp. 121–128, Jan. 2014.

[12] J. W. Jang, J. S. Kim, O. H. Kwon, T. H. Lee, and Y. S. Cho "UV-curable silicate phosphor planar films printed on glass substrate for white light-emitting diodes," *Opt. Lett.*, vol. 40, no. 16, pp. 3723–3726, Aug. 2015.

[13] Z. Luo, H. Chen, Y. Liu, S. Xu, and S.-T. Wu, "Color-tunable light emitting diodes based on quantum dot suspension," *Appl. Opt.*, vol. 54, no. 10, pp. 2845–2850, Apr. 2015.

[14] M.-H. Shin, H.-G. Hong, H.-J. Kim, and Y.-J. Kim, "Enhancement of optical extraction efficiency in white LED package with quantum dot phosphors and air-gap structure," *Appl. Phys. Exp.*, vol. 7, no. 5, p. 052101, May 2014.

[15] J.-H. Kim, W.-S. Song, and H. Yang, "Color-converting bilayered composite plate of quantum-dot–polymer for high-color rendering white light-emitting diode," *Opt. Lett.*, vol. 38, no. 15, pp. 2885–2888, Aug. 2013.

[16] J. Y. Woo, K. Kim, S. Jeong, and C.-S. Han, "Enhanced photoluminance of layered quantum dot–phosphor nanocomposites as converting materials for light emitting diodes," *J. Phys. Chem. C*, vol. 115, no. 43, pp. 20945–20952, Nov. 2011.

[17] J. H. Kim and M. W. Shin, "Thermal behavior of remote phosphor in light-emitting diode packages," *IEEE Electron Device Lett.*, vol. 36, no. 8, pp. 832–834, Aug. 2015.

[18] R. Hu, X. Luo, and H. Zheng, "Hotspot location shift in the high-power phosphor-converted white light-emitting diode packages," *Jpn. J. Appl. Phys.*, vol. 51, no. 9S2, p. 09MK05, Sep. 2012.

[19] K.-J. Chen *et al.*, "The influence of the thermal effect on CdSe/ZnS quantum dots in light-emitting diodes," *J. Lightw. Technol.*, vol. 30, no. 14, pp. 2256–2261, Jul. 15, 2012.

[20] A. Shi, X. Wang, X. Meng, X. Liu, H. Li, and J. Zhao, "Temperature-dependent photoluminescence of $CuInS_2$ quantum dots," *J. Lumin.*, vol. 132, no. 7, pp. 1819–1823, Jul. 2012.

[21] L. Yin, Y. Bai, J. Zhou, J. Cao, X. Sun, and J. Zhang, "The thermal stability performances of the color rendering index of white light emitting diodes with the red quantum dots encapsulation," *Opt. Mater.*, vol. 42, pp. 187–192, Apr. 2015.